

A Unified Modeling Approach using Bond Graph Method and its Application for Model Order Reduction and Simulation

Engr. Lubna Moin (e-mail engr_lubna@yahoo.com)
 Dr. Vali Uddin (e-mail v_uddin@hotmail.com) National
 University of Sciences & Technology Pakistan Navy
 Engineering College Karachi

ABSTRACT

Bond graph is the methodology for modeling multidisciplinary dynamic system. They are succinct pictorial statements of mathematical modeling. The traditional modeling and simulation techniques for dynamic systems are generally adequate for single-domain systems only, but the Bond Graph technique provides new strategies for reliable solutions of multi domain system. They are also used for analyzing linear, non linear dynamic production system, artificial intelligence, image processing, robotics and industrial automation. They are domain independent, allow free composition and are efficient for classification and analysis of model, allowing repaid determination of various types of acceptability or feasibility of candidate design.

This research introduces an approach to model order reduction that retains structural information in the reduced order model. Neither traditional methods such as aggregation nor modern techniques that explain H_∞ theory maintains a link between the structure of the original model and the reduced order model. In other words, the state variables and the coefficients of the ROM have no connection to the state variables of the original model. In contrast the algorithm developed in this research derived from the Bond Graph, maintains a subset of original state variables in ROM and maintains structural significance in the state variable coefficients.

Key words: Bond graph modeling, multi-domin system, model order reduction, mechatronic systems, simulation

1 INTRODUCTION

The traditional modeling and simulation techniques for dynamic systems are generally adequate for single domain systems only. Mechatronic systems being a mixture of mechanical and electric systems, deal with multi-domain system. Such systems may typically include translational, rotational, thermo fluid, electrical, electric mechanical and electric system. Modeling and Simulation of such multi-domain systems pose formidable new challenges and hence demand new strategies and techniques for reliable studies, BOND GRAPH method (BGM) is rapidly emerging to offer a new modeling and simulation methodology that is ideally suited to effectively unify knowledge pertaining to multi domain systems for mechatronics applications[12].

The BGM combined with genetic programming (GP) offers tremendous opportunities in artificial

intelligence, image processing and robotic and industrial automation.

The extension of BGM for applications to fields such as social behavior, economics and operational research is a very active topic of current research[1].

In the our research work, we have used this Bond graph technique for model order reduction, we have introduced an approach to model order deduction that sustains structural information in the reduction order model (ROM). The approximation of high-order plant and controller model by models of lower order is an integral part of control systems design. For model order reduction we have used balanced reduction truncation, Hankel norm, Schmidt method and bond graph elimination of elements[11].

Standard approach to model-order reduction eliminate any connection between the state variables of the original and reduced-order models. When the state

variables and state matrix coefficients of the original model are physically based, the loss of this structure is unfortunate. Model order reduction that is intended to provide insight into the system simultaneously obscures the physical significance of the state variables and the coefficients of the state matrices. Thus while standard approaches to model order reduction do address the issue of model error vs. model order, they do not help a designer decide which physical state variables should be included in a model[17].

This research addresses the problem of determining which physical state variables should be retained in a reduced order model that belongs to a class of lumped physical system models, the class is defined by SISO variable pair of systems that are passive and free of internal loops. The model synthesized in this thesis are intended primarily for controller design, and will be expressed using bond graphs. An error term that describes the reduced order model frequency response uncertainty over a given frequency range of interest is also provided.

This thesis builds on recent work in synthesizing and analyzing tree-structured transfer functions which have the form of a continued fraction. A useful feature of this transfer function is the manner in which it allows state variables to be easily removed from a model

Note that a subset of existing model reduction methods are also based on continued fraction. However, these methods all require that a continued fraction expansion to be performed on the without considering the physical structure of the model. The continued fraction representation found in this paper, is a tree-structured decomposition (TSD), which is facilitated by bond graph theory. The original model is symbolic, and a unique TSD results. Furthermore, in this paper, model order reduction is accomplished by physically-based approximations, as opposed to truncating continued fraction terms. Hence, the proposed method should not be confused with traditional methods, even though they may both employ continued fractions.

The technique is applied on two different systems. One is an mechanical system, a lumped model of a DC motor, with four wheels and three complaint torsional shafts. The algorithm and other model reduction techniques are secondly applied to 11th order high pass filter.

The model order reduction process with both system indicates which system component have the most bearing on the frequency response and secondly the final model retains the structural information.

2. LITERATURE REVIEW

2.1 Modeling of the system by bond graph method

Bond graph is an explicit graphical tool for capturing the common energy structure of systems. It increases one's insight into systems behavior. In the vector form, they give concise description of complex systems. Moreover, the notations of causality provides a tool not only for formulation of system equations, but also for intuition based discussion of system behavior, viz. controllability, observability, fault diagnosis, etc [10].

2.1.1 Bond Graph Standard Elements

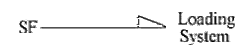
In bond graphs, one needs to recognize only four groups of basic symbols, i.e., three basic one port passive elements, two basic active elements, two basic two port elements and two basic junctions. The basic variables are effort (e), flow (f), time integral of effort (P) and the time integral of flow (Q)[10].

2.1.1.1 Basic 1-Port elements

A 1-port element is addressed through a single power port, and at the port a single pair of effort and flow variables exists. Ports are classified as passive ports and active ports. The passive ports are idealized elements because they contain no sources of power. The inertia or inductor, compliance or capacitor, and resistor or dashpot are classified as passive elements. The active ports are those, which give reaction to the source. For, example if we step on a rigid body, our feet reacts with a force or source. For this reason, sources are called active ports. Force is considered as an effort source and the surface of a rigid body gives a velocity source. They are represented as an half arrow pointing away from the source symbol. The effort source is represented by



and the flow source is represented as shown below.



In electrical domain, an ideal shell would be represented as an effort source. Similarities can be drawn for source are presentations in other domains.[12].

Table 1: This table presents bond graph symbols and the consecutive relations for sources.

	Bond Graph System	Defining Relation
Generalized	$S_e \square$	$e(t)$ given, $f(t)$ arbitrary
Variables	$S_f \square$	$f(t)$ given, $e(t)$ arbitrary
Mechanical	$S_v \square$	$F(t)$ given, $V(t)$ arbitrary
Translation	$S_t \square$	$V(t)$ given, $F(t)$ arbitrary
Mechanical rotation	$S_m \square$	$\tau(t)$ given, $\omega(t)$ arbitrary
Hydraulic	$S_Q \square$	$P(t)$ given, $Q(t)$ arbitrary
Systems	$S_e \square$	$Q(t)$ given, $P(t)$ arbitrary
Electrical	$S_t \square$	$e(t)$ given, $i(t)$ arbitrary
Systems		$i(t)$ given, $e(t)$ arbitrary

2.1.1.2 Basic 2-Port elements

There are only two kinds of two port elements, namely "Transformer" and "Gyrator". The bond graph symbols for these elements are TF and GY, respectively. As the name suggests, two bonds are attached to these elements. The bond graphic transformer can represent an ideal electrical transformer, a mass less lever, etc. The transformer does not create, store or destroy energy. It conserves power and transmits the factors of power with proper scaling as defined by the transformer modulus. A transformer relates flow-to-flow and effort-to-effort. Conversely, a gyrator establishes relationship between flow to effort and effort to flow, again keeping the power on the ports same. The simplest gyrator is a mechanical gyroscope.

2.1.1.3 The 3-Port junction elements

The name 3-port used for junctions is a misnomer. In fact, junctions can connect two or more bonds. There are only two kinds of junctions, the 1 and the 0 junction. They conserve power and are reversible. They simply represent system topology and hence the underlying layer of junctions and two-port elements in a complete model (also termed the Junction Structure) is power conserving. 1 junctions have equality of flows and the efforts sum up to zero with the same power orientation.

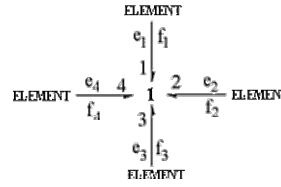


Figure 1: 1 junction

0 junctions have equality of efforts while the flows sum up to zero, if power orientations are taken positive toward the junction.

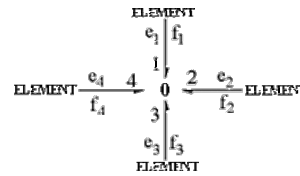


Figure 2: 0 junction

2.1.2 Assigning numbers to bonds

The bonds in a bond graph may be numbered sequentially using integers starting with 1. However, one need not follow any fixed rule. Assignment of bond number also fixes the name of the elements or junctions. This is the best bookkeeping technique adopted by most of the existing software products. Some software though follow numbering of elements according to their instance. However, in models using fields, where many bonds are connected to an element, such a nomenclatures cause difficulty in book-keeping.

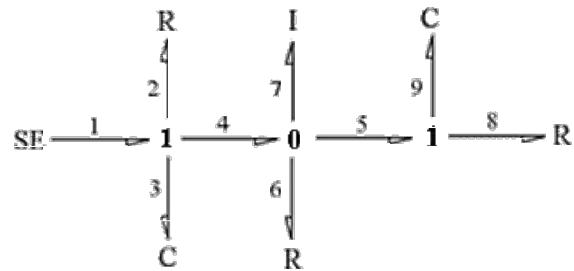


Figure 3: Bond Graph of an RLC Circuit

For example, the two 1-junctions in the bond graph shown in the right can be uniquely identified as (S 1 2 3 4) and (S 5 8 9); similarly symbols like C3, C9 can be used to identify a particular element

2.2 Model order reduction and truncation

The approximation of high-order plant and controller models by models of lower order is an integral part of control system design. It may also be possible to replace high-order controllers by low-order approximations with little sacrifice in performance.

2.2.1 State-space truncation

Consider a linear, time-invariant system with the realization.

$$\dot{x} = Ax + Bu, \quad x(0) = x_0, \quad (1)$$

$$y = cx + Du \quad (2)$$

and divide the state vector x into components to be retained and components to be discarded.

$$x = \begin{bmatrix} x_1 \\ \square x_2 \end{bmatrix} \quad (3)$$

The r -vector $x_1(t)$ contains the components to be retained, which the $(n - r)$ vector x_2 contains the components to be discarded. Now partition the matrices A, B and C conformably with x to obtain.

$$\begin{aligned} A &= \begin{bmatrix} A_{11} & A_{12} \\ \square A_{21} & A_{22} \end{bmatrix}, & B &= \begin{bmatrix} B_1 \\ \square B_2 \end{bmatrix} \\ C &= [C_1 \quad C_2] \end{aligned} \quad (4)$$

By omitting the states and dynamics associated with $x_2(t)$, we obtain the lower-order system.

$$\begin{aligned} \dot{p} &= A_1 p + B_1 u & p(0) &= p_0, \\ q &= C_1 p + Du. \end{aligned}$$

The r^{th} -order truncation of the realization (A, B, C, D) is given by

$$(A, B, C, D) = (A_{11}, B_1, C_1, D) \quad (5)$$

In general, very little can be said about the relationship between x and p, y and q or the transfer function

matrices G and $\overset{3}{G}$ associated with (A, B, C, D) and (A_{11}, B_1, C_1, D) . In particular, the truncated system may be unstable even if the full-order system is stable, and the truncated system realization may be minimal even if the full-order realization is non minimal. One thing that clearly does hold is

$$\overset{3}{G}(\infty) = G(\infty)$$

State-space truncation is a simple but general procedure for generating reduced-order models. The properties of the reduced-order model will depend on the realization selected for truncation. For example, reduced-order models obtained from the truncation of balanced and model realizations (of the same full-order system) will generally be quite different.

State-space truncation produces zero error at infinite frequency.

Since the singular perturbation method of model truncation is related to state-space truncation by the bilinear transform $s \rightarrow 1/s$, singular perturbation approximations have zero steady-state error.

2.2.2 Balanced model reduction

A realization (A, B, C, D) is balanced if A is asymptotically stable and

$$A\Sigma + \Sigma A + BB = 0 \quad (6)$$

$$A\Sigma + \Sigma A + C C = 0, \quad (7)$$

In which

$$\square = \begin{bmatrix} f_1 & 0 & 0 \\ 0 & \square & 0 \\ 0 & 0 & f_m I_m \end{bmatrix}, \quad f_1 = \dots = f_i = \dots = f_j \text{ and } f_i > 0 \square$$

Note

that $n - \square r_1 + L + r_m$ is the McMillan degree of $C(sI - \square A) \square B$ and that r_i is the multiplicity of f_i . We say that the realization is an ordered balanced realization if, in addition, $f_1 > f_2 > L > f_m > 0$.

In a balanced realization, the basis for the state space is such that each basis vector is equally controllable and observable, with its “degree” of controllability and observability given by the corresponding diagonal entry of Σ .

A balanced realization is an asymptotically stable and minimal realization in which the controllability and observability gramians are equal and diagonal. Any stable transfer function matrix has balanced realization. The balanced realization is unique up to ordering of the number \int_i and an orthogonal transformation that commutes with Σ . An analysis of the extent to which states are involved in energy transfer from past inputs to future outputs motivates the consideration of the balanced realization as an appropriate realization for absolute-error model reduction.

2.2.3 Hankel Operators and Schmidt decomposition
 The Hankel operator maps inputs that are nonzero only negative time to the future part of the output. The rank of the Hankel operator Γ_G is equal to the McMillan degree of its symbol G . The Hankel norm is the square root of the energy gain from inputs that are only nonzero in negative time to the future part of the output.

The Hankel norm is no greater than the infinity norm. Indeed,

$$\|G\|_H \leq \|G - F\|_\infty \quad (8)$$

for any anticausal system F . If $F \in RH_\infty$, then F is anticausal.

The singular values of the Hankel operator Γ_G are given by

$$\sigma_i(G) = \lambda_i^{\frac{1}{2}}(PQ) \quad (9)$$

in which P and Q are the controllability and observability gramians of a minimal realization of G .

The Schmidt decomposition is a singular value decomposition of the Hankel operator Γ_G . The Schmidt vectors are easily determined from a state-space realization of G .

The Hankel norm of the error incurred in approximating G by a system \tilde{G} of McMillan degree r is at least as large as $\sigma_{r+1}(G)$. If this lower bound is attained, $\Gamma_G v_{r+1} = 0$ for any Schmidt vector v_{r+1} corresponding to $\sigma_{r+1}(G)$.

3 MODEL ORDER REDUCTION BY BOND GRAPH METHOD

The modeling framework in this paper assume that a relatively high order bond graph truth model is available. The term relatively high order implies that the model order may be higher than necessary, and the term truth implies that this is the model against which others can be compared. Such a model results when a designer identifies all possible, within reason, candidate energy storage elements (generalized inductances and capacitances) in a physical system and synthesizes a bond graph model of the same. This is a logical scenario: rather than guessing, perhaps incorrectly, which energy elements should be included in the model, the designer simply includes all reasonable elements in the model.

In this thesis the original model has order n and is denoted by $G(s)$. reduced order models of order r are denoted by $G_r(s)$. the multiplicative uncertainty associated with a reduced order model is subscripted by the same parameter, e.g. $w_r(j\omega)$. The reduced order

model and the uncertainty between it and the original model will be characterized in the following manner:

$$G_r = \{\tilde{G}_r(s) \mid \tilde{G}_r(s) = (1 + \Delta(s))G_r(s), \sup_{\omega \in \mathbb{R}} |\Delta(j\omega)| \leq 1\} \quad (10)$$

where

$\omega_r(s)$ a fixed, proper, and strictly stable transfer function, $\Delta(s)$ is a strictly stable transfer function, Unstable and imaginary axis poles of $G(s)$ are not cancelled in forming $\tilde{G}_r(s)$.

The formulation is the well known multiplicative representation for unstructured uncertainty, even though in this case the original model has no uncertainty. The original model is contained in (13) in the sense that

$$G(j\omega) \in G_r(j\omega) \text{ for } \omega \in \Omega, \quad (11)$$

where Ω is the frequency vector $[\omega_1 \ \omega_2 \ \dots \ \omega_m]$.

3.1 Model order reduction algorithm

In bond graph theory, each independent energy storage element requires a state variable, the quantity of which determines the order of the model. Removing most energy storage elements, however, will generally cause model order to decrease by two. For example, when the compliance that separates masses m_2 and m_3 in Fig.30 is removed, it is replaced by a rigid, inertialess member. The two masses become rigidly coupled, and a single state variable describes their momentum. Thus, removing a single compliant element decreases model order by two, one for the compliance elements displacement and one for a momentum. Removing an inertia that is between two compliant elements

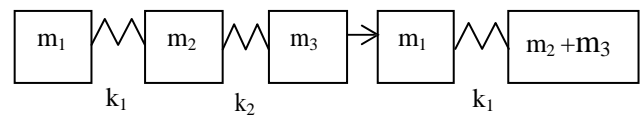


Figure 4: removing compliance k_2 from a model

Associated with the armature winding of a DC motor only reduces model order one.

An unnecessary energy element is one whose removal causes only a marginal change in model performance for excitations over the FROI. If a given energy storage element meets this criteria, there is little motivation to keep it in the model, and it should be removed. A series of steps are required to identify an unnecessary energy storage element. Although these steps apply at any stage of model order reduction, they are more readily explained by beginning with the original full order

model. The procedure to identify the first unnecessary energy storage element follows.

1. Number the energy storage elements from $i = 1$ to n , let $i = 1$
2. Remove energy storage element i from the model
3. Synthesize the corresponding reduced order transfer function, $G_r^i(s)$
4. Using $G_r^i(j\omega)$ and $G(j\omega)$, determine the corresponding error $e_r^i(j\omega)$,
5. Repeat #2 #4 for the remaining elements

6. Find the energy storage element whose removal causes the smallest error, if this error, e_r , is below some tolerance, this element is unnecessary. Note that elements needed for input and outputs cannot be removed from the model. For example, an inertial element with either an effort or a flow input or a flow output must be retained in the model. Similarly, a spring whose effort is an output must be kept in the model. Other elements may also need to be retained in the model if they receive an input or are used to obtain an output.

Synthesizing a reduced order model, Step 3 from above, can be accomplished using a tree-structured transfer function or conventional $\{A,B,C,D\}$ matrices, both obtainable from a bond graph. However, as the same tree-structured transfer function can be used repeatedly in step 3, it is preferable to use this transfer function, rather than synthesize a new set of state matrices at each step. To illustrate, let us consider a model of original order n and a final model of order r . furthermore, assume that each order reduction step reduces model order by two. The total quantity of model needed to synthesize $G_r(s)$ equals

$$n \times (n - 2) \times (n - 4) \times \dots \times r. \quad (12)$$

Clearly it is preferable to use the same transfer function to obtain this quantity of model, rather than to synthesize the same quantity of realizations.

The uncertainty term caused by the removal of a given energy storage element, step 4, is provided by the quantity

$$e_r^i(j\omega) = \left| \frac{G_r^i(j\omega)}{G(j\omega)} \right|. \quad (13)$$

The error in Step 6 is determined by the maximum error over the entire FROI

$$e_r^i = \max_{\omega} e_r^i(j\omega).$$

The energy storage element whose removal causes the smallest change is thus determined by

$$i_{\min,r} = \arg \min e_r^i$$

3.2 Properties of the reduced order model

By following the algorithm, a reduced order model $G_r(s)$ and a vector of errors $\{e_r(j\omega)\}$ are obtained. The original full order model, $G(j\omega)$, is used to determine $e_r(j\omega)$, which in turn is used to find the lower bound of the magnitude of the multiplicative uncertainty:

$$\left| \frac{e_r(j\omega)}{G_r(j\omega)} \right| \leq \frac{e_r(j\omega)}{|G_r(j\omega)|} \quad (14)$$

Once a proper and strictly stable transfer function, $w_r(s)$, is found that satisfies (12), the following set inclusion is guaranteed:

$$G(j\omega) \subseteq \tilde{G}_r(j\omega) \quad (15)$$

where $\tilde{G}_r(s)$ is defined in (13). Therefore, the reduced order model with multiplicative uncertainty on the RHS of (14) can be used to design controllers for the full order model. Not that the intent of this thesis is not to find a multiplicative uncertainty transfer function that satisfies (18). Rather, the goal is to develop a procedure for synthesizing a reduced order model that does not significantly increase the error, $e_r(j\omega)$, in (18). Once this error is available, the transfer function $w_r(j\omega)$ can be synthesized.

The order of the model was reduced using four methods, and maximum absolute errors were determined as a function of model order. The methods included the bond graph approach developed here, balanced model reduction, the Hankel norm approximation and H_∞ norm model approximation with prescribed eigen values.

4 Application of the Approach for Modeling and Model Order Reduction

The Bond Graph approach for Modeling and Model Order Reduction applied to two different systems.

4.1 Example of a Mechanical System

DC Motor with Fly Wheels and Torsional Shafts
 A lumped of a DC motor, four flywheels, and three compliant torsional shafts is shown in Fig.6. although not shown in the figure, the flywheels are supported by bearings which impart viscous friction to the flywheels. The shafts are assumed to have no structural damping which is a conservative assumption.

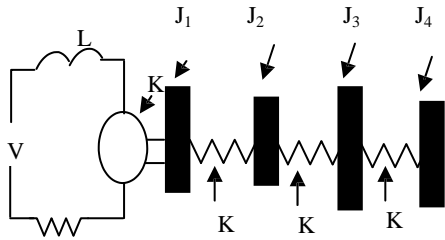


Figure 5: Dc Motor with Fly Wheel and Torsional Shafts

4.1.1 Bond graph Representation

A bond graph of the lumped model in Fig. is shown in Fig. .

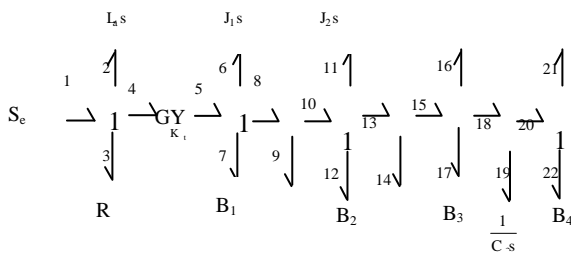


Figure 6: Bond Graph of Dc Motor with Fly Wheel and Torsional Shafts

4.1.2 Synthesis of Tree-Structured Transfer Function

Tree-structured transfer functions result from replacing typical bond graph elements with their impedance equivalents, specifying impedance-laws for bond graph multiports, and recursively substituting element impedances into the impedance-law terms. In mechanical translational systems impedance is the force divided by velocity; in electrical systems impedance is the voltage divided by current. Other physical domains have their own definitions of impedance. Basic bond graph elements, their constitutive laws and their impedance equivalents are provided in Table 1, where f represents generalized flow, e represents generalized effort, z represents impedance, and s represents the Laplace variable. In addition to the elements impedances, gyrator and transfer function impedance equivalents are

also available. The impedance of the second bond reflected to the first bond equals

$$z_1 = r^2 z_2 \quad \square, \text{ (gyrator impedance law)} \quad (16)$$

Table 2: Elements and their impedances

Element	Constitutive Law	Impedance (z)
Resistance	$e = Rf$	$\frac{e}{f} = R$
Capacitance	$\int f = Ce$	$\frac{e}{f} = \frac{1}{C_s}$
Inertia	$\int e = If$	$\frac{e}{f} = I_s$

$$z_1 \begin{matrix} \square \\ \text{GY} \\ \square \end{matrix} \begin{matrix} \square \\ z \\ \square \end{matrix} \quad 2$$

$$1 \begin{matrix} \square \\ z \\ \square \end{matrix} \begin{matrix} \square \\ \text{TF} \\ \square \end{matrix} \begin{matrix} \square \\ z \\ \square \end{matrix} \quad 2$$

where z_1 represent the impedance of a given bond. For the transformer, the impedance of the second bond reflected to the first bond equals

$$z_1 = m^2 z_2. \text{ (transformer impedance law)} \quad (17)$$

Multiport impedance equivalents can also be derived. These equivalents are used to synthesize a dynamic system. Here the intent is to synthesize a transfer function with a tree (continued fraction) structure. The impedance equivalents are developed by applying the well-known flow and effort laws for one-junctions and zero junctions. Bonds attached to the one junction share a common flow, and the efforts of the bonds attached to this junction sum to zero. For one junction we have

$$\sum_i e_i = 0, \quad (18)$$

where efforts associate with half arrows directed towards a junction are given positive values and those associated with arrows directed away from a junction are given negative values. When each of these efforts is divided by the flow f associates with the one-junction, which is the same for all attached bonds, the following impedance law results:

$$\boxed{f}_i \frac{e}{f} = \boxed{e}_i \frac{f}{e} = \boxed{z}_i = 0. \quad (\text{one junction impedance law}) \quad (19)$$

law) (19)

In the case of a zero-junction the attached bonds share a common effort, and the flows of the bonds sum to zero. For zero-junction we have

$$\boxed{f}_i = 0, \quad (20)$$

where flows associated with half-arrows directed towards a junction are given positive values and those associated with arrows direct away from a junction are given negative values. When each of these flow is divided by the effort e associated with the junction, which is same for all attached bonds, the following impedance law is obtained:

$$\frac{\boxed{f}_i}{e} = \boxed{f}_i \frac{1}{e} = \boxed{z}_i = 0. \quad (\text{zero junction impedance law}) \quad (21)$$

We seek the transfer function that relates the voltage input to the angular velocity of the first flywheel. This is a common transfer function, where the plant is driven by a power amplifier and the motor tachometer is used as the output sensor. To synthesize a tree-structured transfer function of $\omega_1(s) / V_{in}(s)$, we begin by defining the element impedances in the bond graph.

$z_2=L_a s, \quad z_2= R_a, \quad z_6= J_{1s}, \quad z_7= B_1, \quad z_9= 1/C_{1s}$ and so on.

The gyrator impedance equivalence is provided in (1). Applied to the bond graph, this relation results in

$$z_4 = \frac{K_t^2}{Z_5} \quad (22)$$

Applying the one-junction impedance equivalence, to the bond graph results in

$$\begin{aligned} z_1 &= z_2 + z_3 + z_4 & z_5 &= z_6 + z_7 + z_8 \\ z_{10} &= z_{11}z_{12}+z_{13} & z_{15} &= z_{16} + z_{17} +z_{18} \\ z_{20} &= z_{21} + z_{22} \end{aligned}$$

Lastly, applying the above to the bond graph provides,

$$\begin{aligned} z_8 &= (z_9 + z_{10}) & z_{13} &= (z_{14} + z_{15}) & z_{18} &= (z_{19} + z_{20}) \end{aligned} \quad (23)$$

In terms of bond graph variables, the transfer function $\omega_1(s)/V_{in}(s)$ equals f_6/e_1 . To obtain this ratio in terms of impedances, we perform the following sequence of operations

$$\frac{\omega_1(s)}{V_{in}(s)} = \frac{f_6}{e_1} = \frac{f_6}{f_5} \frac{f_5}{e_4} \frac{e_4}{f_4} \frac{f_4}{f_1} \frac{f_1}{e_1} = 1 \cdot \frac{1}{K_t} \cdot z_4 \cdot 1 \cdot \frac{1}{z_1} \quad (24)$$

By substituting the element impedance into the equivalences in (6) and (7) and working from the right of the bond graph in fig.28 towards the left, we obtain

$$\begin{aligned} z_1 &= L_a s + R_a + z_4 \\ z_4 &= \frac{K_t^2}{J_1 s + B_1 + \frac{1}{\frac{s}{K_1} + \frac{1}{J_2 s + B_2 + \frac{1}{\frac{s}{K_2} + \frac{1}{J_3 s + B_3 + \frac{1}{\frac{s}{K_3} + \frac{1}{J_4 s + B_4}}}}}}} \end{aligned}$$

Expressed as a conventional ratio of polynomials, (10) has an eighth order denominator. For the equivalent {A,B,C,D} realization of $\omega_1(s)/V_{in}(s)$, we begin by defining the statevector

$$x = [\begin{matrix} \theta_1 \\ \theta_2 \\ \theta_3 \\ \theta_4 \end{matrix}]^T \quad \text{TM}_1 \text{ TM}_2 \text{ TM}_3] ,$$

where $\theta_i = L_a i_a$ and TM_i represent the angular springs in Fig. The A matrix for displacement of the this plant is:

		0	0	0	0	0	0	0
$-R_a/L_a$	$-K_t$							
K_t/J_1	$-B_1/J_1$	0	0	0	0	0	0	0
0	0	B_2/J_2	0	0	K_1/J_2	0	0	0
0	0	0	$-B_3/J_3$	0	0	K_2/J_3	$-K_3/J_3$	0
0	0	0	0	$-B_4/J_4$	0	0	0	$-K_3/J_4$
0	0	-1	0	0	0	0	0	0
0	0	1	-1	0	0	0	0	0
0	0	0	1	-1	0	0	0	0

4.1.3 Plant parameters and frequency range of interest

The system in Fig. is parameterized by the following values:

$L_a = 0.0030$	$R_a = 0.9000$	$J_1 = 0.011$	$B_1 = 3.9167 \times 10^{-4}$
$J_2 = 7.6377 \times 10^{-3}$	$B_2 = 2.3860 \times 10^{-4}$	$J_3 = 0.0010$	$B_3 = 2.3860 \times 10^{-4}$
$J_4 = 7.6451 \times 10^{-5}$	$B_4 = 2.3860 \times 10^{-4}$	$K_1 = 0.0600$	$K_t = 0.237$
$K_2 = 38.1590$	$K_3 = 23.617,$		

where SI units are used through. Substituting these values in (11) results in the following pole-zero vectors:

$$P = [-0.262 -299.6 - 0.114 \pm 7.01j - 0.214 \pm 198j - 1.44 \pm 578j]$$

$$Z = [-4.10 \times 10^{-2} \pm 5.21j - 0.215 \pm 198j - 1.44 \pm 578j]$$

For this example we will assume that the FROI is bound by [1, 50]. Initially the vector Ω is defined by 400 logarithmically spaced frequency grid points. The S_e vector is augmented by the imaginary values of the poles and zeros in (180 that in the range [1, 50].

The order of the models were reduced using four methods and maximum absolute errors were determined as a function of model order. The methods included the bond graph approach, balanced model reduction, the Hankel Norm approximate and Schmidt method of model reduction.

4.2 Example of an Electrical System 11th order high pass filter

A filter design problem was used as a test of over approach for evolving electrical circuit with bond graphs. The first phase we desired its bond graph using the theoretical background stated previously.

4.2.1 Bond graph representation

A filter design problem was used as a test of over approach for evolving electrical circuit with bond graphs. The first phase we desired its bond graph using the theoretical background stated previously.

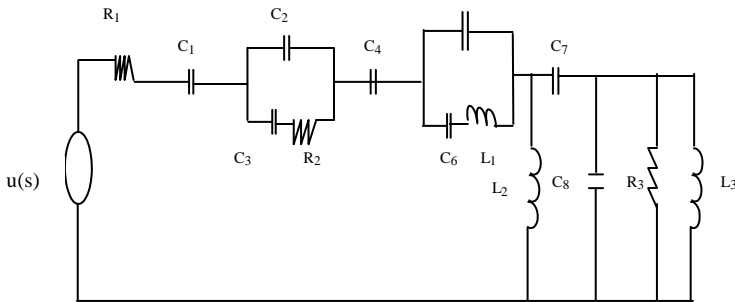


Figure 7: 11th Order high Pass Filter

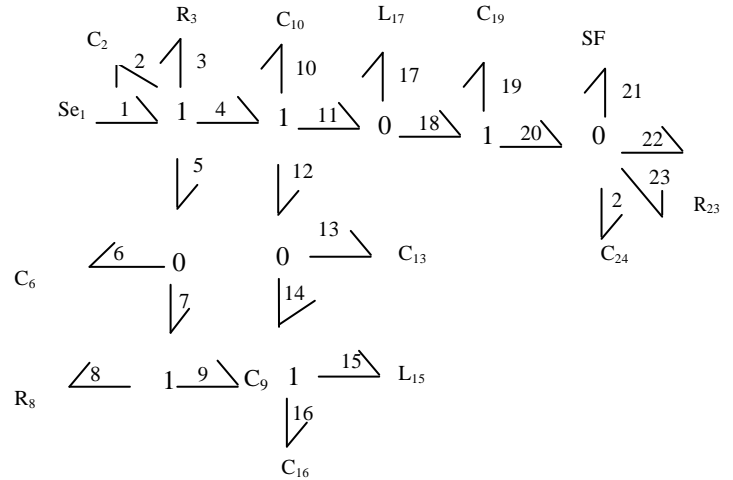


Figure 8: Bond Graph of 11th Order high Pass Filter

4.2.2 Deriving state space representation from Bond Graph

The energy variable are,

$$q_{12}, q_6, q_9, q_{10}, q_{13}, q_{16}, q_{19}, q_{24}, p_{17}, p_{15} \text{ and } p_{22}$$

The Co-energy variable are

$$V_1(t), V_2, V_6, V_9, V_{10}, V_{13}, V_{16}, V_{19}, V_{24}, f_{15}, f_{17}, \text{ and } f_{22}.$$

Now

$$\dot{q}_2 = \frac{S_e}{R_3} \square \frac{1}{C_2 R_3} q_2 \square \frac{1}{C_{10} R_3} q_{10} \square \frac{1}{C_{19} R_3} q_{19} \square \frac{1}{C_{24} R_3} q_{24} \square \frac{1}{C_{13} R_3} q_{13} \square \frac{1}{C_6 R_3} q_6 \quad (25)$$

2nd State

$$\dot{q}_6 = \frac{S_E}{R_3} \square \frac{1}{C_2 R_3} q_2 \square \frac{1}{C_{10} R_3} q_{10} \square \frac{1}{C_{19} R_3} q_{19} \square \frac{1}{C_{24} R_3} q_{24} \square \frac{1}{C_{13} R_3} q_{13} \square \frac{1}{C_6 R_3} q_6 \square \frac{1}{C_9 R_8} q_9 \quad (26)$$

3rd State

$$\dot{q}_9 = \frac{1}{C_6 R_8} q_6 \square \frac{1}{C_9 R_8} q_9 \quad (27)$$

4th state

$$\dot{q}_{10} = q_2 \quad (28)$$

5th state

$$\dot{q}_2 = \frac{S_e}{R_3} \frac{1}{C_2 R_3} q_2 \frac{1}{C_{10} R_3} q_{10} \frac{1}{C_{19} R_3} q_{19} \frac{1}{C_{24} R_3} q_{24} \frac{1}{C_{13} R_3} q_{13} \frac{1}{C_6 R_3} q_6 \frac{1}{L_{17}} p_{17} \quad (29)$$

6th state

$$\dot{q}_2 = \frac{S_e}{R_3} \frac{1}{C_2 R_3} q_2 \frac{1}{C_{10} R_3} q_{10} \frac{1}{C_{19} R_3} q_{19} \frac{1}{C_{24} R_3} q_{24} \frac{1}{C_{13} R_3} q_{13} \frac{1}{C_6 R_3} q_6 \frac{1}{L_{15}} p_{15} \quad (30)$$

7th state

$$\dot{q}_{16} = \frac{1}{L_{15}} p_{15} \quad (31)$$

8th state

$$\dot{q}_2 = \frac{S_e}{R_3} \frac{1}{C_2 R_3} q_2 \frac{1}{C_{10} R_3} q_{10} \frac{1}{C_{19} R_3} q_{19} \frac{1}{C_{24} R_3} q_{24} \frac{1}{C_{13} R_3} q_{13} \frac{1}{C_6 R_3} q_6 \frac{1}{L_{17}} p_{17} \frac{1}{L_{22}} p_{22} \frac{1}{C_{24} R_{23}} q_{24} \quad (32)$$

9th state

$$\dot{p}_{15} = \frac{1}{C_{13}} q_{13} = \frac{1}{C_{16}} q_6 \quad (33)$$

10th state

$$\dot{p}_{17} = \frac{1}{C_{19}} q_{19} \frac{1}{C_{24}} q_{24} \quad (34)$$

11th state

$$\dot{p}_{22} = \frac{1}{C_{24}} q_{24} \quad (35)$$

Hence the state equations are derived from the bond graph.

In the 2nd phase we used the MATLAB programming to evaluate the frequency prepares to the filter original model and then proceed toward the order reduction by elementary the components from the bond graph. The Model order Reduction is also performed for a given Frequency Range of Interest.

4.2.3 Selecting a frequency range and grid

The frequency range of interest (FROI) is of considerable importance in systems engineering, and provides a context within which to formulate requirement on model performance, the FROI is the frequency band $[\omega_{min}, \omega_{max}]$ over which a model, in terms of steady-state input-output predication, should give a reliable indication of system response. Zero is often the lower bound of the FROI. The upper bound may be determined inputs or disturbance inputs specification, e.g., if the frequency content of commanded input or disturbance inputs is known then the model should be accurate to frequency 2-5 times the highest input frequency (W_{in}) accordingly,

$$\omega_{max} = 5 \times \omega_{in}$$

the case of closed-loop system design, the open-loop

In crossover frequency drives the FROI in that the model

decades beyond the crossover frequency ω_{co} . That is,

$$10 \times \omega_{co} \leq \omega_{max} \leq 100 \times \omega_{co}$$

In addition to choosing the FROI, a grid of frequencies over this must also be selected. A uniform grid of say, 10-20 points per decade serves as a staring point. However, frequencies that correspond to the poles and zeros of the

three other modern techniques, balanced realization, Hankel norm and Schmitt technique.

Instead of terminating the reduction process when the error become large, reduction continued until the order is minimum possible. The absolute error between the original and reduction order model for all four methods are then tabulated and sketched.

5 Results

The results thus obtained in the research work are as follows,

1. An integrated tool set for modeling, design and specification is applied.
2. The bond graph for a lumped model of a DC motor with four fly wheels and three complaint torsional shafts is obtained.
3. Tree structure transfer function results from replacing typical bond graph elements with their impedance equivalents, specifying impedance laws for bond graph multiports and recursively substituting element impedance into the impedance-laws terms.
4. Bond graph model for an eleventh high pass filter is obtained and thereafter the transfer function is determined.
5. The order of the models were reduced using four methods and maximum absolute errors were determined as a function of model order. The methods included the bond graph approach, balanced model reduction, the Hankel Norm approximate and Schmidt method of model reduction.
6. Instead of terminating the reduction process when the error become large , reduction continued until the the minimum possible order was obtained. The absolute error between the graph and reduced order models for all four methods are tabulated in tables 5 and 6.
7. The maximum error between the original and reduced order model for all four methods are plotted over the entire frequency range of interest.
8. Hence the research leads towards a new approach of modeling using Bond Graph and Model Order Reduction.

5.1 Matlab programming

La=0.003;

```

Ra=0.900;
J1=0.011;
B1=0.00039167;
J2=0.00763;
B2=0.00023860;
J3=0.0010;
B3=0.0002386;
J4=0.000076451;
B4=0.00023860;
Kt=0.0600;
K1=0.237;
K2=38.1590;
K3=23.617
%entering the matrice of the model
A=[-Ra/La -Kt 0 0 0 0 0; Kt/J1 -B1/J1 0 0 0 -K1/J1 0 0;0 0
-B2/J2 0 0 K1/J2 -K2/J2 0;0 0 0 -B3/J3 0 0 K2/J3 -K3/J3 ;0
0 0 0 -B4/J4 0 0 K3/J4; 0 1 -1 0 0 0 0;0 0 1 -1 0 0 0;0 0 0
1 -1 0 0 0];
s=[1 0 0 0 0 0 0 0];
B=transpose(s);
C=[0 0 1 0 0 0 0 0];
D=0;
sys=ss(A,B,C,D)

% Balanced Model Reduction

[ar1,br1,cr1,dr1,er1,hsv1]=balmr(A,B,C,D,1,7);
[ar2,br2,cr2,dr2,er2,hsv2]=balmr(A,B,C,D,1,6);
[ar3,br3,cr3,dr3,er3,hsv3]=balmr(A,B,C,D,1,5);
[ar4,br4,cr4,dr4,er4,hsv4]=balmr(A,B,C,D,1,4);
[ar5,br5,cr5,dr5,er5,hsv5]=balmr(A,B,C,D,1,3);
[ar6,br6,cr6,dr6,er6,hsv6]=balmr(A,B,C,D,1,2);
[ar7,br7,cr7,dr7,er7,hsv7]=balmr(A,B,C,D,1,1);

% Frequency adjustment

% for w=.1 to 100
%w=logspace(-1,2,400);
%w(1,154)=1.4110;
%w(1,327)=28.4569;
%w(1,360)=50.0545;
%w=w(1,134:359);

% for w = 1 to 50

w=logspace(0,2,300);
w(1,23)=1.4110;
w(1,218)=28.4569;
w=w(1,1:255);

% Magnitude

[mp,pp]=bode(A,B,C,D,1,w);
[mp1,pp1]=bode(ar1,br1,cr1,dr1,1,w);
[mp2,pp2]=bode(ar2,br2,cr2,dr2,1,w);
[mp3,pp3]=bode(ar3,br3,cr3,dr3,1,w);
[mp4,pp4]=bode(ar4,br4,cr4,dr4,1,w);
[mp5,pp5]=bode(ar5,br5,cr5,dr5,1,w);
[mp6,pp6]=bode(ar6,br6,cr6,dr6,1,w);

```

```
[mp7,pp7]=bode(ar7,br7,cr7,dr7,1,w);
```

```
% residual
```

```
[ar11,br11,cr11,dr11]=parallel(ar1,br1,cr1,dr1,A,B,-C,D);
[mp11,pp11]=bode(ar11,br11,cr11,dr11,1,w);
mpres1=mp11./mp;
err1= max(mp11)
errres1=max(mpres1);
```

```
[ar22,br22,cr22,dr22]=parallel(ar2,br2,cr2,dr2,A,B,-C,D);
[mp22,pp22]=bode(ar22,br22,cr22,dr22,1,w);
mpres2=mp22./mp;
err2= max(mp22)
errres2=max(mpres2);
```

```
[ar33,br33,cr33,dr33]=parallel(ar3,br3,cr3,dr3,A,B,-C,D);
[mp33,pp33]=bode(ar33,br33,cr33,dr33,1,w);
mpres3=mp33./mp;
err3= max(mp33)
errres3=max(mpres3);
```

```
[ar44,br44,cr44,dr44]=parallel(ar4,br4,cr4,dr4,A,B,-C,D);
[mp44,pp44]=bode(ar44,br44,cr44,dr44,1,w);
mpres4=mp44./mp;
err4= max(mp44)
errres4=max(mpres4);
```

```
[ar55,br55,cr55,dr55]=parallel(ar5,br5,cr5,dr5,A,B,-C,D);
[mp55,pp55]=bode(ar55,br55,cr55,dr55,1,w);
mpres5=mp55./mp;
err5= max(mp55)
errres5=max(mpres5);
```

```
[ar66,br66,cr66,dr66]=parallel(ar6,br6,cr6,dr6,A,B,-C,D);
[mp66,pp66]=bode(ar66,br66,cr66,dr66,1,w);
mpres6=mp66./mp;
err6= max(mp66)
errres6=max(mpres6);
```

```
[ar77,br77,cr77,dr77]=parallel(ar7,br7,cr7,dr7,A,B,-C,D);
[mp77,pp77]=bode(ar77,br77,cr77,dr77,1,w);
mpres7=mp77./mp;
err7= max(mp77)
errres7=max(mpres7);
```

```
diary vv1
```

```
disp('          Balanced Model Reduction')
disp('          -----')
```

```
disp(' ')
disp([' Order ' ' MaxError ' ' ResidualError ' '
RelativeResidualError'])
disp(' ')
disp([7 er1 err1 errres1;6 er2 err2 errres2;5 er3 err3 errres3;4
er4 err4 errres4; 3 er5 err5 errres5;2 er6 err6 errres6;1 er7
err7 errres7])
```

```
diary off
```

```
semilogx(w,20*log10(mp),'r-
',w,20*log10(mp1),'gx',w,20*log10(mp2),'m-
',w,20*log10(mp3),'b-',w,20*log10(mp4),'y-
',w,20*log10(mp5),'c-',w,20*log10(mp6),'g-
',w,20*log10(mp7),'bo');
grid
```

```
% Final results
```

```
% original plant = [A,B,C,D]
```

```
% reduced order plant
```

```
% seventh order=[ar1,br1,cr1,dr1]
% sixth order=[ar2,br2,cr2,dr2]
% fifth order=[ar3,br3,cr3,dr3]
% fourth order=[ar4,br4,cr4,dr4]
% third order=[ar5,br5,cr5,dr5]
% second order=[ar6,br6,cr6,dr6]
```

```
% magnitudes
```

```
% mp original plant
% mp1 seventh order plant
% mp2 sixth order
% mp3 fifth order
% mp4 fourth order
% mp5 third order
% mp6 second order
% mp7 first order
% Absolute error
```

```
% mp11 seventh order plant
% mp22 sixth order
% mp33 fifth order
% mp44 fourth order
% mp55 third order
% mp66 second order
% mp77 first order
```

```
% Relative error
```

```
% mpres1 seventh order plant
% mpres2 sixth order
% mpres3 fifth order
% mpres4 fourth order
% mpres5 third order
% mpres6 second order
% mpres7 first order
```

```
% m file to plot the absolute error of the modified plant
model using
% different model reduction techniques
% Final results
% modified 10-9-04
```

```

cla
order1=[1 2 3 4 5 6 7 8];

herror=[0 3.0999e-2 1.6318e-7 3.1732e-2 7.102e-7 3.0919e-2
1.7411e1 1.7082e1];
balerror=[0 7.6136e-13 1.0056e-12 1.651e-7 1.5619e-9
2.0569e-2 1.1471e1 1.1361e1];
hanerror=[0 2.6314e-10 3.6608e-8 5.5329e-7 1.11422e-6
2.0569e-2 1.2156e1 1.124e1];

order2=[1 3 5 6 8];
bonderror=[0 3.0314e-4 3.3104e-2 1.5057e-1 1.1355e1];

semilogy(order1,balerror,'rx',order1,herror,'bo',order1,hanerro
r,'g*');
legend('Balanced Model Reduction','H-Infinity Norm Model
Approximation','Hankel Norm Model Reduction','Bond
Graph Method');
hold
semilogy(order1,balerror,'r-',order1,herror,'b-
',order1,hanerror,'g-',order2,bonderror,'m-');
set(gca,'xticklabels',[8 7 6 5 4 3 2 1])
xlabel('Order');
ylabel('Absolute Error');
grid
hold off
    
```

5.2 Reduced Order Model Errors for Mechanical System

Table 3: Reduced Order Model Errors for Mechanical System

Order	Absolute Error				Component Removed
	Balanced	H _∞	Hankel Norm	Bond Graph	
8	0	0	0	0	
7	7.61 × 10 ⁻¹³	3.09 × 10 ⁻²	2.63 × 10 ⁻¹⁰	na	
6	1.01 × 10 ⁻¹²	1.63 × 10 ⁻⁷	3.66 × 10 ⁻⁸	3.03 × 10 ⁻⁴	K ₃
5	1.65 × 10 ⁻⁷	3.17 × 10 ⁻²	5.53 × 10 ⁻⁷	na	
4	1.56 × 10 ⁻⁹	7.10 × 10 ⁻⁷	1.11 × 10 ⁻⁶	3.31 × 10 ⁻²	K ₂
3	2.06 × 10 ⁻²	3.09 × 10 ⁻²	2.06 × 10 ⁻²	1.51 × 10 ⁻¹	L _a
2	11.4	17.4	12.1	na	
1	11.4	17.4	11.2	11.3	K ₁

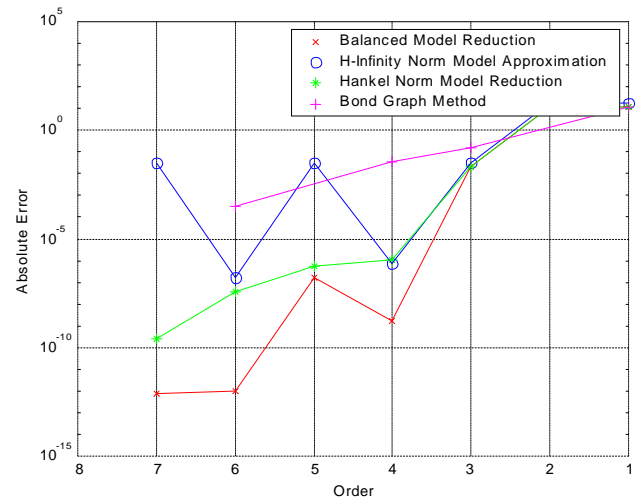


Figure 9: Absolute error as a function of Model Order

5.3 Reduced order Model Errors for Electrical System

Table 4: Reduced order Model Errors for Electrical System

Order	Absolute Error				Component Removed
	Balanced	Hankel Norm	Schmidt	Bond Graph	
11	0	0	0	0	0
10	1.6713e-013	1.3556e-009	1.7959e-010	8.2747e-018	C2
9	1.7153e-013	2.4386e-008	1.7959e-010	8.2747e-018	C6
8	1.9599e-013	2.4386e-008	1.7959e-010	1.3660e-009	C13
7	4.9048e-011	1.2828e-009	1.796e-010	3.9802e-005	C13, L17
6		2.4386e-008	2.5026e-008	1.660e-009	C6, C13
5		9.7993e-009	2.3413e-008	1.366e-009	C2, C6, C13, L15
4		9.7993e-009	2.3413e-008	2.2816e-009	C2, C6, C13, L15, L22
3		8.2048e-006	8.1565e-006		
2		4.0157e-004	4.0155e-004		

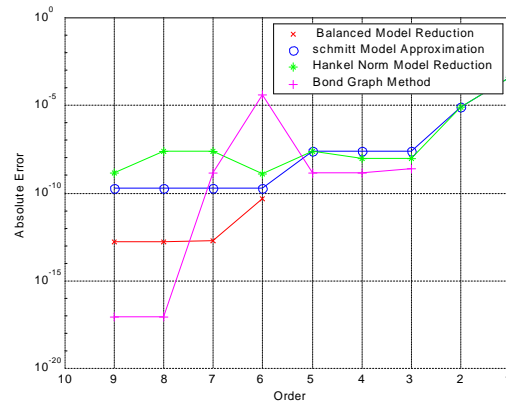


Figure 10: Absolute error as a function of Model Order

4 CONCLUSION

In this research work a new Modeling Approach using Bond Graph Method is applied. It suggested a new design methodology for automatically synthesizing design for multi-domain, lumped parameter dynamic systems, assembled from mixtures of electrical, mechanical, hydraulic, pneumatic and thermal components.

The second conclusion leads toward model order reduction. As the error plot indicates, the discrepancy between the original and reduced order models is smallest when using the balanced model reduction method, followed by the Hankel norm approximation, the H_∞ norm model approximation, and the elimination of physical elements from the model.

The ordering of errors thus obtained is expected. Balanced model reduction, the Hankel norm approximation, and the H_∞ norm model approximation all seek to minimize the absolute error between the original and ROM; the only constraint on this minimization is that the resulting model must be RH_∞ . In contrast to the mathematically-derived models, with the Bond Graph method, the elimination of physical elements from the model constrains the reduced order model to use state variables and coefficients from the original full order model. While we will not use this example to make any definitive claims regarding the efficacy of various order reduction methods, several comments are in order. The example illustrates that the errors resulting from the approach presented here, while generally larger than those encountered from purely mathematical approaches, are not so large as to render the reduced model unusable. The example also indicates that for the Bond Graph method developed here, model error increases monotonically with the amount by which the order has been reduced. In contrast, both balanced model reduction and H_∞ norm model approximation result in non-monotonic behavior for the model error. This suggests another advantage of the new approach, once the model errors have become too large, a user of the algorithm knows there is no point in reducing the order further. The error in Fig.36 & 37, indicate only the maximum error over the entire FROI. For the example here, the Bond Graph method actually produced lower errors than the other methods across the majority of the FROI. The relatively large errors indicate in table 5 and 6 result from model errors that are largely confined to a narrow frequency band within the FROI.

The Model Order Reduction Technique developed in this Thesis has two principal advantages:

1. The Model Order Reduction process indicates which system components have the most bearing on the frequency response.
2. The final model retains structural information.

The first of these features provides a designer with insight in the system behaviour. Where as poles, zeros, the frequency response, and so on simply mathematically derived properties of a model, the order reduction process presented here identifies and eliminates relatively rigid elements from a model. This indicates to a designer that such elements have little bearing on the response within a FROI. As the algorithm is used to identify and eliminate more and more relatively rigid elements, it will eventually become clear which complaint elements are more responsible for the first few resonances in a model.

Therefore, a designer wishing to improve the frequency response of a system, i.e. increase the frequency of a low frequency modes, will know which system elements to modify.

The second feature allows a designer to analyze all the remaining state variables and combination thereof. This is in contrast to other model reduction approaches, which only provide unique input output information. Note, that for exact analysis, the frequency response uncertainty also need to be determined for each output.

7 REFERENCES

- [1] Kohda, T.; Kataube, H.; Fujihara, H.; Inoue, K. "Identification of system failure cases using bond graph models". Conference proceedings. 1993 International Conference on systems, Man and Cybernetics. Systems Engineering in the Service of Humans (Cat. No. 93CH3242-5) p. 269-74 vol.5, IEEE New York, NY, USA. 17-20 Oct 1993.
- [2] Besombes, B.; Marcon, E "Bond-graphs for modelling of manufacturing systems". Conference Proceedings. 1993 International Conference on systems, man and Cybernetics. Systems Engineering in the Service of Humans (Cat. No. 93CH3242-5) p. 256-61 vol.3, IEEE New York, NY, USA. 17-20 Oct 1993.
- [3] Bidard, C.; Favret, F.; Goldztejn, S.; Lariviere, E "Bond graph and variable causality". Conference Proceedings. 1993 International Conference on systems, man and Cybernetics. Systems Engineering in the Service of Humans (Cat. No. 93CH3242-5) p. 270-5 vol.1, IEEE New York, NY, USA. 17-20 Oct 1993.

[4] Delgado, M.; Garcia, J. “ Parametric identification on bond graph models”. Conference Proceedings. 1993 International Conference on systems, man and Cybernetics. Systems Engineering in the Service of Humans (Cat. No. 93CH3242-5) p. 583-8 vol.1, IEEE New York, NY, USA. 17-20 Oct 1993.

[5] Amerongen, J. van and P.C. Breedveld, “Modelling of physical Systems for the Design and Control of Mechatronics Systems”. In IFAC Professional Briefs, published in relation to the 15th triennial IFAC world Congress, International Federation of Automatic Control. Laxenburg, Austria, pp.1-56,2002

[6] D.G. Walker, J.L. Stein, and A.G. Ulsoy. “ Input output criterion for linear model deduction in K.Danai” Proceeding of the ASME Dynamic Systems and Control Division, pages 673-681, Atlanta, GA, 1996. 1996 ASME International Mechanical Engineering Congress and Exposition.

[7] D.Kavranoglu. “Computation of the solution for the H_{∞} model reduction problem”. In proceedings of the American Control Conference, pages 2190-2194, San Francisco, CA 1993

[8] Mayer, R. R., 2001, “Application of Topological Optimization Techniques to Automotive Structural Design”. Proceedings of the ASME 2001 International Mechanical Engineering Congress and Exposition, November 11-16, New York, NY, IMECE 2001/ AMD 25458.

[9]. Uddin, V “A Bond Graph based approach to Model Reduction, Proceedings of the 1998 American Control Conference, Philadelphia, PA, USA. 1998

[10]. Lubna Moin and Dr.Valiuddin “A Unified Modeling Approach using Bond Graph Method and its Application for Model Order Reduction and Simulation” proceedings of 8th multitopic IEEE conference INMIC2004, IEEE catalog number 04EX930, ISBN: 0-7803-8680-9, Library of Congress:2004109608.

[11]. Lubna Moin and Dr.Valiuddin “Application of Tree Structured Transfer Function to an Electromechanical System, it’s comparison with Conventional Method and Application for Order Reduction” Proceedings of CIMCA 2005, IEEE Computer Society Order Number P2504 ISBN-13: 978-0-7695-2504-4 ISBN-10: 0-7695-2504-0, Library of Congress Number 2005935651